RSC Advances

ROYAL SOCIETY OF CHEMISTRY

www.rsc.org/advances

Electrochemical Detection of Azidothymidine on Modified Probes based on Chitosan Stabilised Silver Nanoparticles Hybrid Material

Preeti Tiwari, Ashish Kumar and Rajiv Prakash[*]
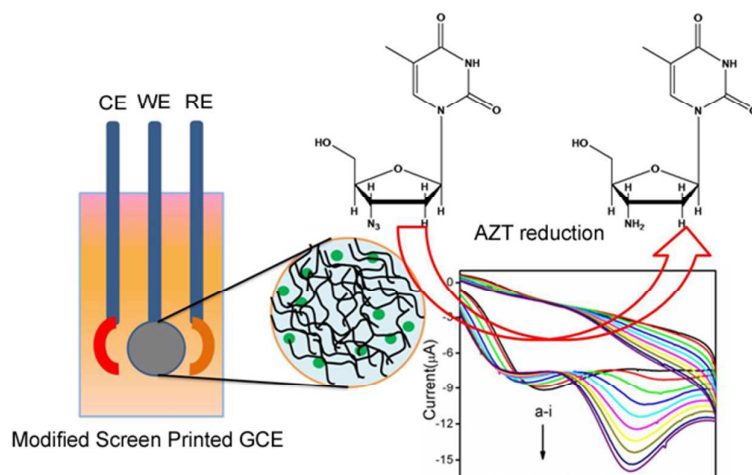
School of Materials Science and Technology, Indian Institute of Technology (Banaras Hindu University), Varanasi-221005, India.

Tel.: +91 9935033011, Fax: +91 542-2368707

[*]Corresponding Author: rprakash.mst@iitbhu.ac.in

Table of contents

Silver nanoparticle stabilized by Chitosan is synthesized for modification of sensing probe for AZT estimation in human plasma.

1

Abstract

Present work deals with the development of Chitosan (Ch) stabilized silver nanoparticles (Ch@Ag NPs) hybrid material modified screen printed graphite electrodes (SPGE) for electrochemical detection of Azidothymidine (AZT). AZT is an antiretroviral (ARV) drug used for the treatment of persons infected with HIV-1. Ch@Ag NPs have been synthesized successfully using one pot chemical synthesis approach. As-synthesized Ch@Ag NPs are characterized by various techniques like UV-vis., Zeta potential, FT-IR, field emission scanning electron microscopy (FESEM), energy dispersive X-ray spectroscopy (EDAX), transmission electron microscopy (TEM) and cyclic voltammetry techniques. This hybrid material is used for the development of sensing probes. Before development of SPGE based sensing probes, first we modified commercial glassy carbon electrode (GCE) by Ch@Ag NPs (Ch@Ag NPs/GCE) in order to check the capability of this hybrid nanomaterial towards electroactivity and detection of AZT. The catalytic effect of this hybrid is explained based on coordination ability with AZT molecules and excellent electroactivity due to the large energetic surface of Ag NPs. Thereafter, modification is extended using Ch@Ag NPs on SPGE (Ch@Ag NPs/SPGE) for developing cost effective portable sensors. As-modified Ch@Ag NPs/GCE has been used for AZT detection in the wide range of concentration from 1.0 μM to 718 μM in 0.1M phosphate buffer solution (PBS, pH=7.6) using voltammetric techniques. Further AZT is also successfully detected over Ch@Ag NPs/SPGE in the concentration range of 10 μM to 533 μM in phosphate buffer solution as well as in biological samples (human Plasma) using simple cyclic voltammetric technique. The limit of detection (LOD) of Ch@Ag NPs/SPGE is found to be 1μM in PBS and 10μM in biological samples (human plasma) at S/N (Signal to noise ratio):3.

Keywords: Azidothymidine, Chitosan, Silver nanoparticle, Cyclic voltammetry, Electrochemical sensing, Hybrid nanomaterial and Screen printed electrode.

1. Introduction

Acquired immunodeficiency syndrome (AIDS) is an immunosuppressive disease, which is caused by HIV-1(Human immunodeficiency virus-1). 3'-azido-3'-deoxythymidine (Zidovudine or Retrovir or Azidothymidine or AZT), a nucleoside reverse transcriptase inhibitor (NRTI), is considered to be safe and effective for curing HIV. It is officially approved and commercialised as retrovir in 1987. AZT is still extensively used as

2

antiretroviral (ARV) drug for the treatment of persons infected with HIV-1 [1-6]. Due to its undesirable side effects and short therapeutic interval, the determination of AZT in human serum is the most important for patient's health. The toxic side effects are generally exhibited when the patient's serum concentration is above 10 μM [7, 8]. Various methods like chromatography [9], radioimmunoassay (RIA) [10], fluorescence spectroscopy, fluorescence polarisation immunoassay (FPIA) [11] and electrochemical technique [12, 13] have been proposed for the determination of AZT. Among these methods, electrochemical technique exhibits great attention due to fast response, high sensitivity and low cost as well as easy development of user friendly appliances and disposable screen printed electrode. In general, the azido group (present in AZT) is considered as an antiviral agent as well as the basis of electrochemical analysis during electrochemical reduction clinically [14-18].

Metal nanoparticles have exhibited great attention due to their significant contribution in wide areas of science and technology including catalysis, photonics, chemical sensor and biosensor [19-22]. Particularly, noble metal nanoparticle like Ag, Au, Pt, Pd, etc. exhibits great attention due to their biostability, high spectral properties and easy functionalisation. Among these metal nanoparticles (NPs), most of the electrochemical sensing is based on Au NPs and Ag NPs [23, 24]. However, the aggregation of nanoparticles restricts their usage as active material for sensors and so far. Therefore, stabilization of these nanomaterials by incorporation of foreign material like polymer, or macromolecules is one of the most common choices to reduce its aggregation. In addition, it is also useful to provide a suitable matrix for modification of sensing probes. For instance, the functionalization of Ag NPs with appropriate molecules like citric acid and phenothiazine, and polymeric matrix like protein, poly [4-(thiophen-3yl)-aniline is of great interest particularly in sensor and catalysis application [22, 25-28]. Chitosan (Ch) is an environmentally friendly biopolymer and considered as an excellent stabilizing agent for nanoparticles due to its biocompatibility, low toxicity and high adsorption properties [29, 30]. Recently, we have demonstrated excellent film formation of metal stabilised Ch for sensing applications [31, 32]. Literature survey exemplifies that most of the work is devoted for AZT detection based on HMDE (Hanging mercury drop electrode) [33-35]. However, few works have been reported based on conducting polymer composite modified graphite paste electrode and Ag-MWCNT composite nanofilm modified glassy carbon electrode [36, 37]. In spite of their advantages, these techniques require complicated processing for AZT detection. At the same time, regeneration of commercial electrode may not be suitable for on-site measurement because its operation is time consuming and requires highly trained users. Therefore, disposable screen

3

printed graphite electrode (SPGE) is one of the best choices to overcome these issues. This is due to its cost effectiveness and easiness in electrode assembly (in a single matt), which make it well suited for mass production of portable devices.

To the best of our knowledge, the utilisation of Ch stabilised Ag NPs modified SPGE portable probe towards electrochemical sensing of AZT is not yet been reported. In this work, we are reporting the development of low cost portable sensors based on Ch@Ag NPs/SPGE probes. Also, the performance of Ch@Ag NPs/SPGE probes have been compared with Ch@Ag NPs modified commercial GCE in buffer and real biological samples.

2. Experimental Details

2.1. Materials

AZT is purchased from Sigma Aldrich, U.S.A. Glacial acetic acid, $AgNO_3$ and Milli Q water are purchased from Merck, India. $NaBH_4$ is obtained from SRL Pvt. Ltd. Chitosan (lower molecular weight Chitosan (poly-(D-glucosamine) =<5400g/mol, degree of deacetylation =84.5%) is brought from Sigma Aldrich. All used reagents are of analytical grade. Phosphate Buffer solution (PBS) of 0.1 M is prepared using NaH_2PO_4 and Na_2HPO_4 (SRL Pvt. Ltd.). All solutions are prepared using double distilled water, and deoxygenated by purging high purity (99.99%) nitrogen gas for 10 minutes prior to each experiment. All experiments are performed at room temperature (25 ºC). Screen printed graphite electrodes (SPGE; WE diameter =2.5 mm, CE and RE width =1.25 mm) are purchased from PalmSens BV, The Netherlands.

2.2. Synthesis of Ch@Ag NPs material

In a typical synthesis of Ch@Ag NPs, 10 mL of 2.5 % stock solution of Chitosan is prepared in 1.0 % acetic acid solution. After that, 2 mL aqueous solution of $AgNO_3$ (17mM) is mixed with 5 mL Chitosan stock solution. Thus prepared solution is kept on stirring for 4 hrs. This mixture is then reduced by 100 μL $NaBH_4$ (0.04 M). The resulting solution is centrifuged and washed several times with Milli-Q water, to remove unreacted $AgNO_3$, NO_3^- and other dissolved impurities. Finally, as-synthesized Ch@ AgNPs is preserved in dark in refrigerator at 4 ºC and used directly for its next experimentations [38].

2.3 Instrumentation

As-synthesized Ch@Ag NPs is characterized for its structural, morphological and electro-chemical properties by means of following instrumental techniques. UV -Vis. spectral changes are observed with Lambda-25 spectrophotometer, Perkin Elmer, Germany. Zeta

4

potential measurement is performed on Nanoparticle Analyzer SZ-100, Japan. FT-IR spectra are obtained using Nicolet 6700 FTIR spectrophotometer, USA. SEM images are taken with the help of FESEM, Curl Zeiss Supra 40, Germany. TE M measurement is executed using HRTEM Tecnai G2, 20 FEI Corporation, the Netherlands operating at 200kV. Voltammetric analysis are performed using CH-instrument (electrochemical workstation, model CH17041C) Inc.USA as well as experiments based on screen printed graphite electrode are executed with PS Trace PalmSens3 (Handheld Potentiostat/ Galvanostat), The Netherlands. Herein former instrument represents reduction with positive current direction while latter instrument represents reduction in negative current direction due to its own default sign convention. Conventional three electrode cell assembly employing GCE or SPGE as working electrode (WE), Pt as counter electrode (CE) and Ag/AgCl as reference electrode (RE) is utilised to study the electrochemical and sensing behaviour. A calibration plot for each sensing measurement is drawn between change in reduction peak current *vs.* AZT concentration in order to determine the LOD and sensitivity of as-fabricated sensing probe. The change in reduction current is calculated by the subtraction of bare current response (without addition of AZT) from actual current response.

2.4 Electrode modification

Prior to the electrode modification, cleaning of commercial GCE (diameter=3.0 mm) and Pt electrode (diameter=3.0 mm) are performed thoroughly using 0.05 μm alumina slurry followed by ultrasonication in ethanol and distilled water sequentially for 10 minutes. Afterwards, 5.0 μL of 2.0 mg Ch@Ag NPs dispersion (in 500 μL distilled water) is drop casted over the commercial GCE (disc diameter =3 mm) and dried in vacuum desiccator. Similar to above procedure, 5.0 μL of 2.0 mg Ch@Ag NPs dispersion (in 500 μL distilled water) is used for the modification of working electrode of SPGE.

3. Results and discussion

The basis of Ch capping on AgNPs in Ch@Ag NPs and its usage as conducting matrix for AZT sensing is shown schematically in scheme I. Various possible interactions between all components are also explained in the scheme I. On addition of calculated amount of Chitosan to acetic acid, protonation of amino group (of Ch) takes place and hence it acts as cationic polymer. Probably a coordination interaction takes place between Ag (I) and electron rich moiety of cationic Ch polymer on addition of aq. $AgNO_3$ in Ch polymer solution [38]. Ch@Ag NPs formed after addition of aq. $NaBH_4$ in above coordinated solution mixture.

5

Similarly, a synergic interaction (between Ag NPs and –OH/C=O: of AZT) was the basis of adsorption of AZT over Ch@Ag NPs matrix. Herein, AgNPs synergistically interact with electron rich functionalities present in Ch matrix as well as AZT (as shown in inset of scheme I). In view of above we tried to exemplify the sensing of AZT over Ch@Ag NPs modified commercial GCE and SPGE experimentally as explained one by one.
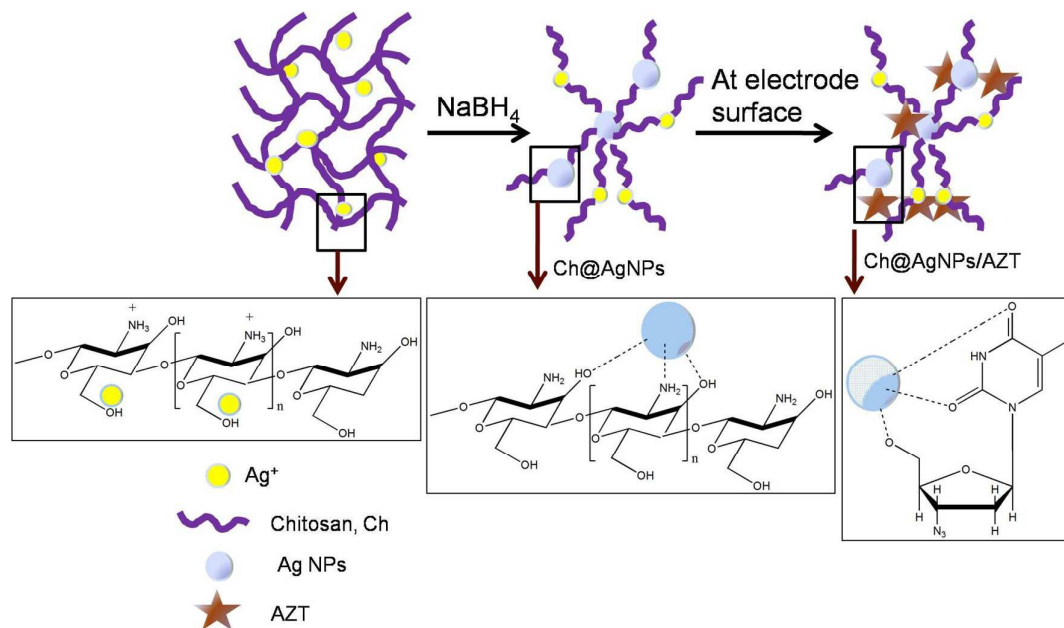
Scheme I: Schematic representation for various interactions between components used for Ch@Ag NPs formation and AZT sensing.

3.1 Characterization of Ch@Ag NPs

3.1.1. UV-vis. Absorption studies

The reduced form of Ag and its interaction with Ch matrix is analyzed by UV- visible absorption spectrum under baseline correction using water to avoid misconceptions related to peak of water (as shown in figure 1). Ch is expected to be a cationic polymer due to protonation of amino group present in the molecule (as it is only soluble in acid) [39]. Therefore, a broad hump near 210 nm is observed due to electronic excitation for electron pair on oxygen (-OH group) of Ch (as shown in inset of figure 1) in UV-visible spectrum. However, as-prepared Ch@Ag NPs shows a broad absorption band at 437 nm for characteristic surface Plasmon resonance of reduced Ag NPs and a new absorption peak at 212 nm indicates interaction of oxygen of Ch with reduced Ag NPs [38]. The Plasmon resonance peak for Ag NPs is size dependent and observed a red shift with increase of particle size [40].
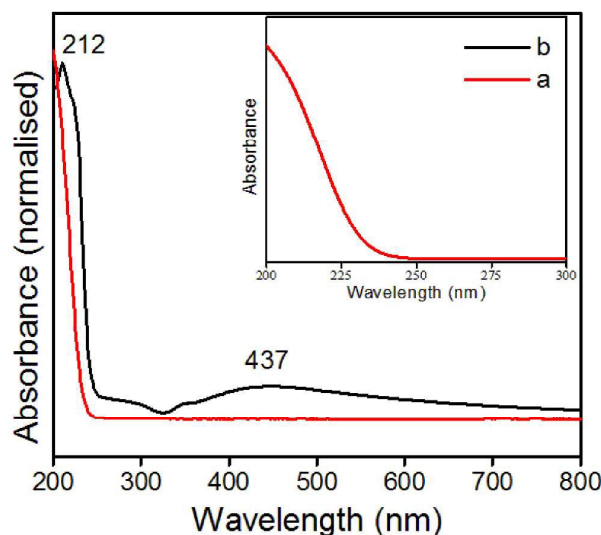
6

Figure1: UV-visible spectra of (a) Ch and (b) Ch@Ag NPs in water. Inset shows zoomed view of Ch from 200 nm to 300 nm.

The dispersion stability of as-prepared Ch@Ag NPs in water is determined spectroscopically by zeta potential (ζ) measurement that indicates the changes occurred on the surface of Ch@Ag NPs with respect to time. For an ideal dispersion, the ζ value more than +30 and-30 is considered to be stable [41]. The ζ value of our as-prepared Ch@Ag NPs is +38.2 mV (figure 2), which indicates its high stability in water over a long period of time.
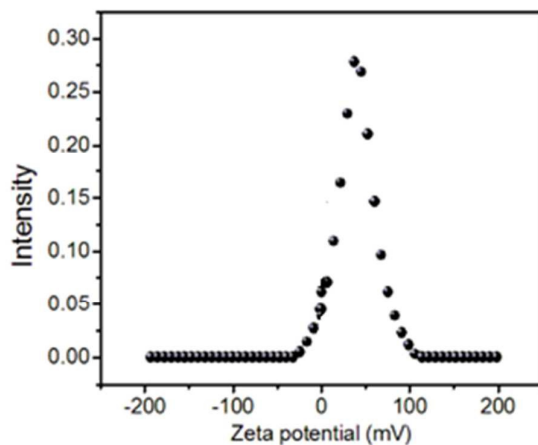

Figure 2: Surface zeta potential graph of Ch@Ag NPs.

3.1.2. FT-IR analysis:

The electrostatic interaction between Ag NPs with the Ch matrix is again investigated by FT-IR as shown in figure 3. In general, Ch exhibits major absorption bands at 891 cm^{-1} and 1152 cm^{-1} that can be attributed to the glycosidic bonding [42]. The characteristics bands at 3433

7

cm^{-1} (stretching vibration of –OH and –NH groups), 2879 cm^{-1} (symmetric stretching vibration of –CH$_3$ group in amide linkages), 1647 cm^{-1}(stretching vibration of C=O groups), 1420 cm^{-1} (vibration of the primary alcoholic group) and 1574 cm^{-1} (bending vibration of N-H group) are assigned from the literature as shown in figure 3a [43-45]. However, a decrease in these vibration peaks is observed in case of Ch@Ag NPs. For example the peak at 3433 cm^{-1} shifted to 3420 cm^{-1}, the peak at 1653 cm^{-1} shifted to 1636 cm^{-1} and the peak at 1420 cm^{-1} shifted to 1387cm^{-1} (as shown in figure 3b). These shifts of wave number of stretching and bending vibration of N-H, O-H and symmetric stretching vibration of C=O groups suggest that there is an interaction between Ag NPs and Ch matrix due to transfer of electron density from C and N atoms to the Ag atoms.
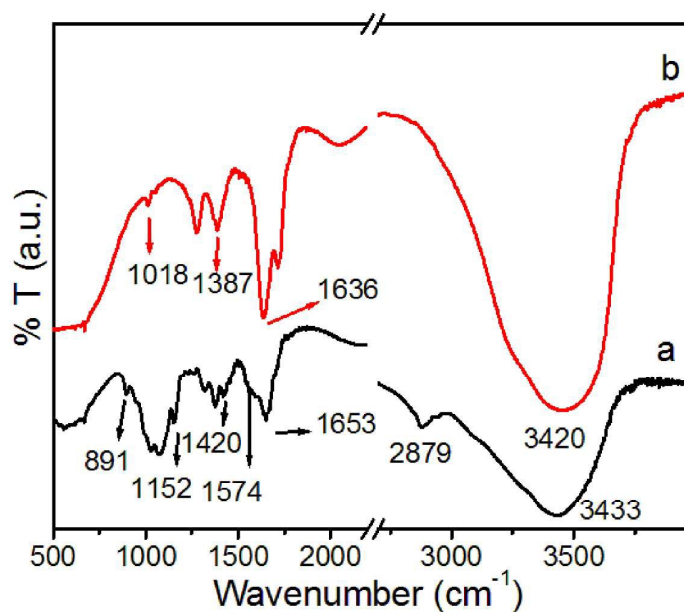

Figure 3: FT-IR spectrum of (a) Ch and (b) Ch@Ag NPs.

3.1.3. EDAX analysis

The reduction of Ag is confirmed by EDAX as shown in figure 4. The EDAX spectrum exhibits that Ch@Ag NPs contains C, N, O and Ag elements with 23.95, 38.44, 3.50 and 34.11 wt. % respectively recorded for enclosed square area. From this spectrum it is exemplified that presence of a strong signal near 3 keV is due to surface Plasmon resonance of metallic Ag [46].
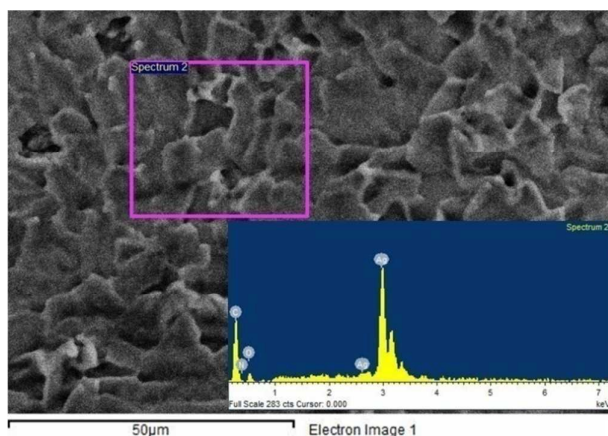
8

Figure 4: EDAX spectrum of Ch@Ag NPs.

3.2 Morphological analysis

The surface texture of Ch and Ch@Ag NPs is analyzed by FESEM images as shown in figure 5. From this figure it is evident that Ch matrix is forming globular, uniform and dense film (as shown in figure 5a) which is holding Ag NPs (as shown in figure 5b).
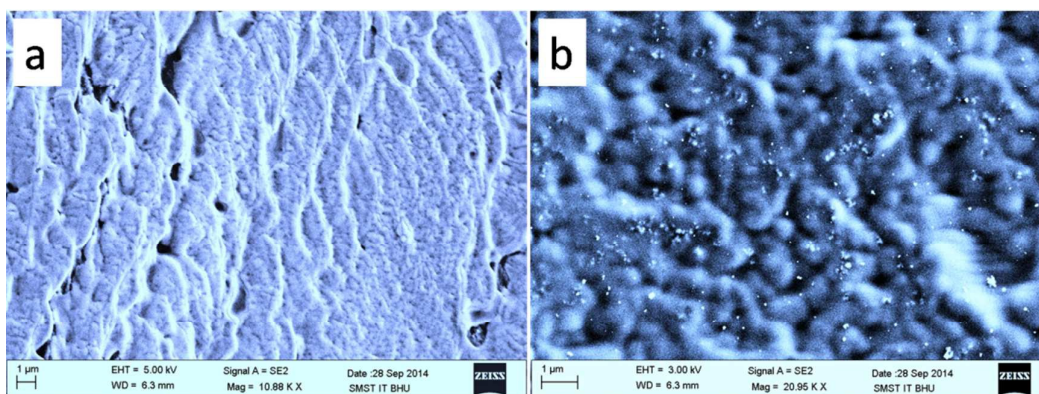

Figure 5: SEM of (a) Ch and (b) Ch@Ag NPs.

These Ag NPs in Ch@Ag NPs exist in its reduced state which is observed by TEM after completion of the reaction (as shown in figure 6a). Herein we observed similar texture of particles as seen earlier by FESEM. These particles exhibit various diffraction patterns corresponding to reduced Ag as observed by selected area electron diffraction (SAED) pattern (as shown in figure 6b). From this pattern it can be concluded that Ag NPs are crystalline in nature showing Scherrer rings corresponding to (111), (200) and (220) planes of *fcc* lattice. The average particle size distribution of as-prepared Ch@Ag NPs lies in nanometric range from 25 nm to 45 nm calculated from figure 6a using standard Image J software (shown in figure 6c).
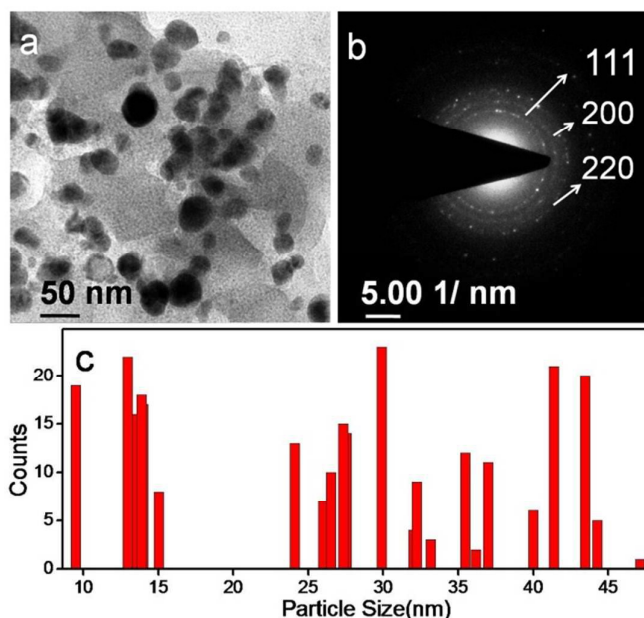
9

Figure 6: (a) TEM image, (b) SAED pattern and (c) particle size distribution of Ch@Ag NPs.

3.3 Electrochemical analysis of AZT

In general interpretation, the electrochemical reduction behaviour of AZT is observed due to the presence of azido group. The azide group exhibits electro-reduction that depends on pH of the medium used for analysis. When medium is alkaline, the reduction is proposed via $2H^+$ and four electron transfer processes [47]. In above view, commercial GCE, commercial Ag electrode and as-modified Ch@Ag NPs/GCE are checked carefully first for its electro-chemical activity towards AZT reduction and then, applied for various concentration of AZT determination. The stepwise experimentations are described as follows:

Prior to AZT detection, Ch@Ag NPs/GCE is checked for its redox behaviour and compared with commercial GCE by performing CV in PBS (pH=7.6) as shown in figure 7. It exhibits Ag oxidation peak at +0.34 V and its corresponding reduction peak at -0.026 V. However, such type of redox behaviour is not observed in case of bare commercial GCE (*cf.* figure 7a and figure 7b). After that, Ch@Ag NPs modified electrode is compared with macro electrodes i.e. commercial Ag and GCE at a fixed concentration for the AZT reduction as shown in figure 8. In this experiment, 5.0 µL of 2.0 mg Ch@Ag NPs dispersion (in 500 µL distilled water) is loaded over commercial GCE and compared with bare GCE and commercial Ag electrode for its electrochemical response (CV) towards AZT reduction. On comparing the reduction peaks of AZT, we observed that Ch@Ag NPs/GCE successfully gives reduction peak for AZT at -0.60 V (*cf.* figure 8b and figure 8c). However, this peak

10

shifts towards positive side (-0.45 V) in case of commercial Ag electrode. The shift in peak potential of modified electrode is probably due to insulating nature of Chitosan film. Herein more energy input is required due to insulation or high impedance of the electrode in case of Ch modification. Further, the catalytic effect of modified electrode is observed in terms of peak current when difference in reduction current (Δi) is calculated for two different concentrations of AZT solution (295µM and 439 µM) by performing CV at fixed scan rate for both the electrodes i.e. modified and commercial Ag electrodes. We observed Δi=1.44 µA for commercial Ag and Δi=2.24 µA for Ch@Ag NPs/GCE, indicating catalytic effect of Ch@Ag NPs/GCE. This catalytic effect is due to coordination of AZT with modified electrode and large energetic surface of Ag NPs (shown in supporting information, SI, section [A]). After that Ch@Ag NPs/GCE is again checked for its time dependent reliability during the course of AZT reduction. Herein we observed constant peak voltage and current initially for more than 10 cycles and then goes on decreasing gradually at constant reduction potential due to its poisoning effect (see SI, section [B]).
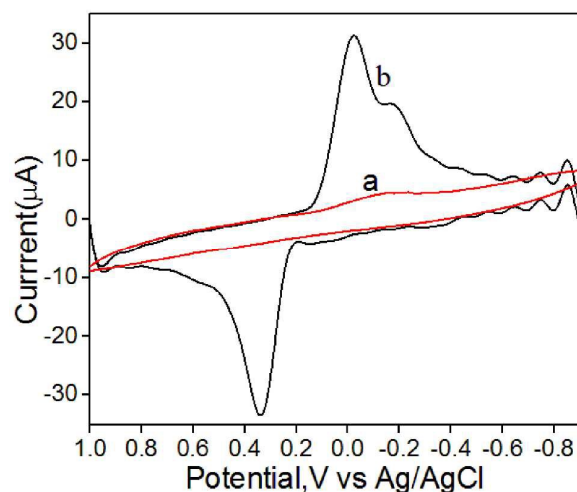

Figure 7: CV of (a) Commercial GCE and (b) Ch@Ag NPs/GCE in 0.1 M PBS (pH 7.6).
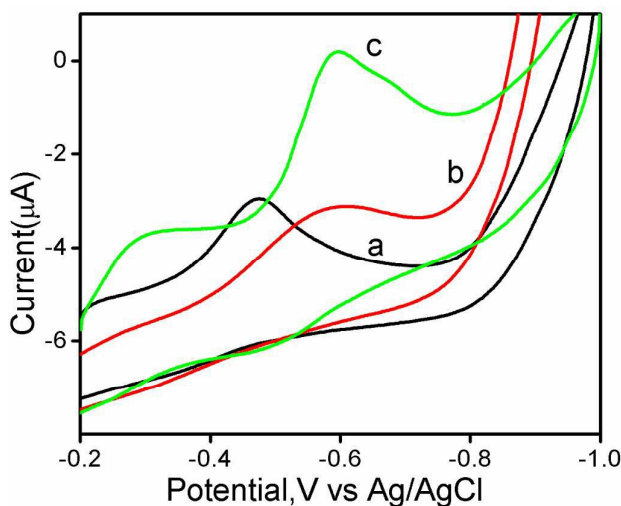
Figure 8: CV of (a) bare commercial Ag electrode, (b) bare commercial GCE and (c) Ch@Ag NPs/GCE in presence of AZT in 0.1 M PBS (pH =7.6).

3.3.1 Effect of scan rate

The electron transfer characteristics of Ch@Ag NPs/GCE is checked and compared with commercial GCE and commercial Ag electrodes at different scan rate ranging from 10 to 500 mV/s (as shown in Figure 9a-c). From these voltammogram, it is evident that the reduction peak current of AZT increases in a linear fashion with the increasing value of square root of scan rate in all cases but with different slopes (as shown in figure 9d). It means that the electrochemical reduction of AZT on Ch@Ag NPs/GCE is diffusion controlled process and depicts fast electron transfer rate as compared to bare commercial GCE and commercial Ag electrode. The fast electron transfer rate is due to high electro-catalytic effect and larger surface area of Ch@Ag NPs. The shift of reduction peak potential of AZT towards more negative value with increasing scan rate reveals the irreversibility of electrochemical reduction of azido group of AZT [47]. Thus, 50 mV/s scan rate is optimized for studying the electrochemical reduction process as the reduction peak appearance is well defined with low over potential of AZT.
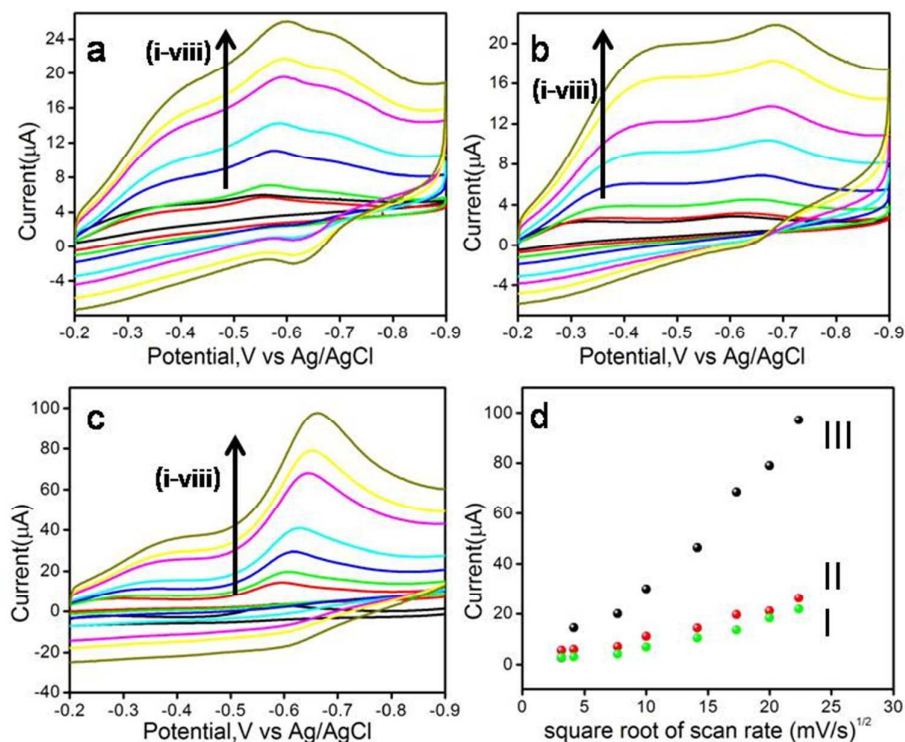
12

Figure 9: CV of (a) commercial GCE, (b) commercial Ag electrode, (c) Ch@Ag NPs/GCE at different scan rates from (i) 10, (ii) 20, (iii) 50, (iv)100, (v) 200, (vi) 300, (vii) 400 and (viii) 500 mV/s in 0.1 M PBS (pH 7.6) and (d) plot of reduction current vs. square root of scan rate of (I) commercial Ag, (II) commercial GC electrode and (III) Ch@Ag NPs/GCE.

On the basis of above speculation, the electrochemical detection of AZT is carried out at various concentrations (above than 10 µM concentration which is toxic for human beings) over Ch@Ag NPs/GCE and Ch@Ag NPs/SPGE at pH=7.6 one by one as explained below.

3.3.2 AZT detection in PBS using Ch@Ag NPs/GCE

Ch@Ag NPs/GCE does not exhibit any well defined voltammetric signal in absence of AZT (in blank) in the potential window from -0.2 V to -1.0 V. This window is selected because the electro-reduction of AZT is expected in this range only. When a known amount of AZT is added in the supporting electrolyte (PBS, pH=7.6), a well defined CV response is observed at -0.60 V *vs.* Ag/AgCl due to reduction of AZT. This suggests that the Ch@Ag NPs efficiently catalyses the reduction of AZT over the modified electrode surface. On serial addition of AZT in the concentration range of 74 µM to 718 µM, Ch@Ag NPs/GCE shows substantial increase in reduction peak current owing to the excellent electro-catalytic effect of Ch@Ag

13

NPs (as shown in figure 10I). Herein Ch@Ag NPs/GCE, Ag NPs facilitates fast electron transfer kinetics due to its high electro-conductivity and larger surface area to volume ratio. After ninth serial addition of AZT in supporting electrolyte, we observe a decrease in the reduction peak current which represents the saturation of the electrochemical detection of AZT (as shown in calibration curve, figure 10II) [48].The LOD and sensitivity of as-prepared Ch@Ag NPs/GCE is calculated by CV as 1 µM and 0.01 µA/µM respectively in PBS at S/N (Signal to noise ratio):3. In order to confirm the consistency in this CV results and also quantify the AZT detection at lower concentration level, differential pulse voltammetry (DPV) technique is applied using similar conditions as used for CV (as shown in SI, section [C]). Herein this technique is used to get a Faradic response especially at the faster scan rates [49-51]. We observed consistent results as in CV.
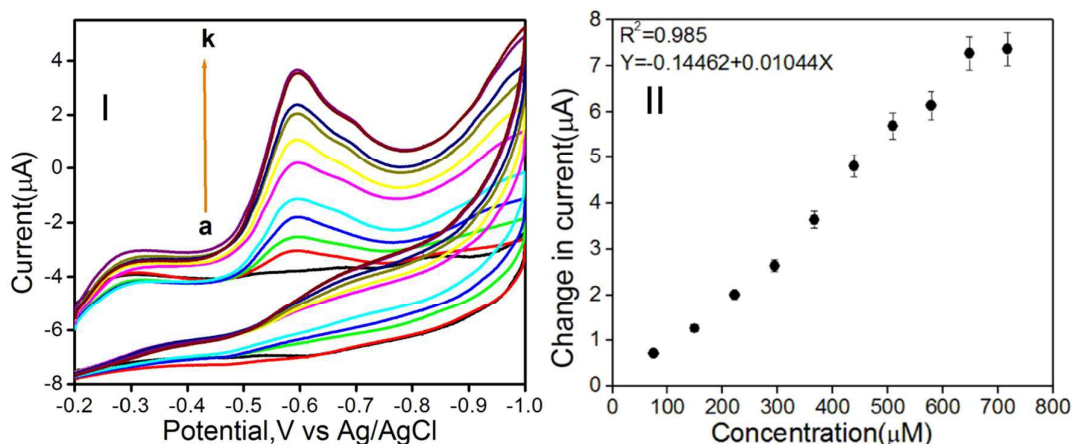

Figure 10: (I) CV response of Ch@Ag NPs/GCE in PBS at pH=7.6 after serial addition of AZT from 74 µM to 718 µM concentration (a-k; a=blank current   b=75 µM, c=149 µM, d=222µ M, e=295 µM, f=367 µM, g=439 µM, h=509 µM, i=579 µM, j=649 µM, k=718 µM) and (II) corresponding calibration plot showing AZT concentration *vs*. Change in reduction current with good correlation coefficient of 0.985.

3.3.3 AZT detection in PBS and human plasma using Ch@Ag NPs/SPGE

After the successful determination of AZT on Ch@Ag NPs/GCE as explained earlier, Ch@Ag NPs material is further used for the modification of SPGE in order to make low cost and portable sensor for the detection of AZT in the concentration range of 10 µM to 533 µM in PBS (pH=7.6) and human plasma (as shown in figure 11). Fresh human plasma solution is used for experimentation purpose with the courtesy of our Institute Hospital. Prior to experimentation, it is diluted four times by deoxygenated high purity N_2 gas (99.99%) 0.1 M, pH=7.6 PBS. We observe similar trend as seen earlier cases, on serial addition of AZT in

14

PBS and in human plasma. The LOD and sensitivity of Ch@Ag NPs/SPGE is 1 μM and 0.015 μA/μM in PBS while it is 10 μM and 0.016 μA/μM in human plasma respectively at S/N: 3.This difference in LOD is probably due to the presence of complex biological matrix in human plasma in comparison to PBS.
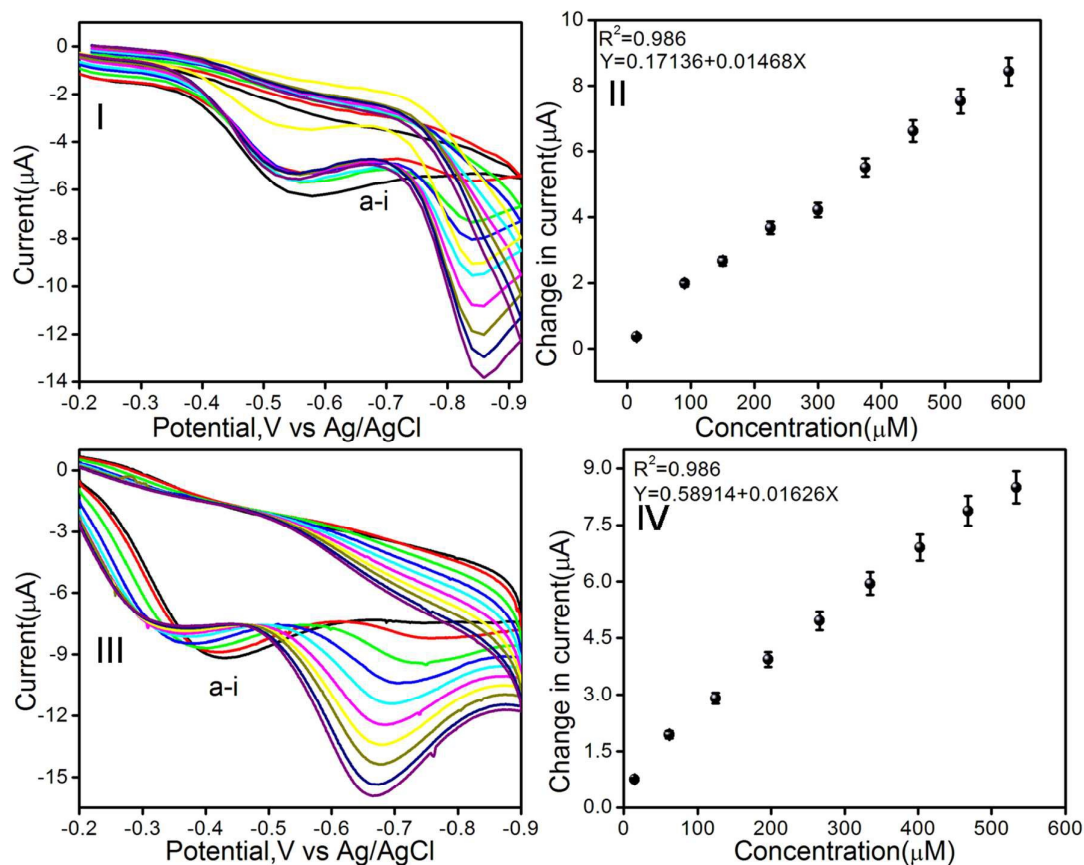

Figure 11: (I) CV response on Ch@Ag NPs/SPGE after serial addition of AZT from 10 μM to 600 μM concentration range (a-i; a=10 μM, b=90 μM, c=150 μM, d=225 μM, e=300 μM, f=375 μM, g=450 μM, h=525 μM, i=600 μM) in PBS at pH= 7.6 with their corresponding calibration plot (II) with good correlation coefficient of 0.986 and (III) CV response on Ch@Ag NPs/SPGCE after serial addition of AZT from 10 μM to 533 μM concentration range (a-i; a=10μM, b=62 μM, c=125 μM, d=195 μM, e=266 μM, f=335 μM, g=403 μM, h=468 μM, i=533 μM) in human plasma at pH= 7.6 with their corresponding calibration plot (IV) with good correlation coefficient of 0.986 (black line represents the blank current).

Simple CV technique is used to lower the cost of portable device and detection of AZT was demonstrated using low cost disposable SPGE up to the toxic level of the AZT (i.e. 10 μM). Further we observe that the Ch@Ag NPs/SPGE does not suffer from electrode poisoning during AZT detection. Our sensing probe showed potential utility of sensor under real

conditions. This sensor exhibits high stability and can be successfully utilised for the fabrication of AZT sensing devices.

Our as-fabricated sensing probe is disposable and cost effective. It has better capability to sense AZT in toxic dose range in human plasma and buffer solution compared to earlier reported works. A comparative study is summarized in table 1 in this context.

Table1: Comparative study for previously reported AZT detections by electrochemical methods.

S. No.	Modified electrode/Ref.	Supporting electrolyte	Reduction potential, V *vs.* Ag/AgCl	Linear response range	AZT detection in real sample	Portable sensor probe
1	HMDE [47]	PBS 0.1M; pH =8	-1.1	500pM-1.0µM	-	-
2	HMDE [12]	PBS 0.1M; pH =8	-0.96	0.4-1500µM	-	-
3	Ag solid amalgam electrode [13]	Borate buffer 0.05M; pH =9.3	-1.05	0.25 to 1.25	-	-
4	Graphite paste electrode [36]	1 mM tris-HCl; pH=6	0.08	1µM-100µM	-	-
5	Ag-NF/M-MWCNT/GCE [37]	PBS 0.1 M; pH= 7	-0.66		Human plasma	-
6	Ch@Ag NPs/GCE and Ch@Ag NPs/SPGE	PBS 0.1M; pH 7.6	-0.60	1µM-718µM	Human plasma	Present Work

4. Conclusion

Ch@Ag NPs hybrid material is synthesized successfully using chemical reduction method involves reduction of Ag salt assisted by NaBH$_4$ in presence of Chitosan as a stabilising agent. This as-synthesized material is well characterized first by various techniques like UV-visible, Zeta potential measurements, FT-IR, SEM, TEM, and EDAX for its structural and morphological properties. We observe that Ch@Ag NPs hybrid material consists of crystalline Ag NPs in Ch matrix which exhibits high dispersion stability in water. Thereafter, it is used as active layer for the fabrication of sensing probes based on commercial GCE and SPGE and applied for AZT detection in toxic dose range (above 10 µM concentration). Electro-reduction of AZT is observed for sensing and detection using voltammetric

16

technique. We observe that the reduction of AZT on modified electrode follows diffusion controlled process. The sensitivity of all electrodes is almost same with different LODs. The LOD of Ch@Ag NPs/GCE and Ch@Ag NPs/SPGE is observed as 1 μM in PBS. Similarly the LOD of Ch@Ag NPs/SPGE is 10 μM in human plasma. Our proposed portable sensor (Ch@Ag NPs/SPGE) is highly reliable for clinical application and laboratory detection of AZT.

Acknowledgement

References:

[1] M.S. Hirsch and R.T. D,Aquila, *N. Engl. J. Med.,* 1993, **328**, 1686-1695.

[2] R.M.W. Hoetelmens, D.M. Burger, P.L. Meenhorst and J.H. Beijnen, *CLIN. Pharmacokinet.,* 1996, **30**, 314-327.

[3] E. Font, O. Rosario. J. Santana, H. Gracia, J.P. Sommadossi and J.F. Rodriguez, *Antimicrob. Agents Chemother.*, 1999, **43**, 2964-2968.

[4] E. De Clercq*, Biochem. Pharmacol.* 1994, **47**, 155-169.

[5] D. Warnke, J. Barreto and Z. Temesgen, *J. Clin. Pharmacol.,* 2007, **47**, 1570-1579.

[6] E. De Clercq*, Future Virol*., 2008, **3**, 393-405.

[7] G.C. Barone III, H.B. Halsall and W.R., Heneman, *Anal. Chim. Acta*, 1991, **248**, 399-407.

[8] Azidothymidine for AIDS, *Med. Lett. Drug Ther.,* 1886, **28**, 726, 107-109.

[9]M. Quevedo, S. Teijeiro and M. Briñón, *Anal. Bioanal. Chem.,* 2006, **385**, 377–384.

[10] G.G. Granich, M.R. Eveland and D.J. Krogstad*, Antimicrob. Agents Chemother.,* 1989, **33**, 1275–1279.

[11] M.A. Raviolo, J.M. Sanchez, M.C. Briñón and M.A. Perillo, *Colloids Surf. B,* 2008, **61**, 188–198.

[12] K.C. Leandro, J.C. Moreira and P.A.M. Farias, *Anal. Lett.,* 2010, **43**, 1951–1957.

[13] K. Pecková, T. Navrátil, B. Yosypchuk, J.C. Moreira, K.C. Leandro and J. Barek, *Electroanalysis,* 2009, **21**, 1750-1757.

[14] L. Trnkova, R. Kizek and J. Vacek, *Bioelectrochem.,* 2004, **63**, 31-36.

[15] D.M. Mattson, I.M. Ahmad, D. Dayal, A.D. Parsons, N.A. Burns, L. Li, K.P. Orcutt, D.R. Spitz, K.J. Dornfeld and A.L. Simons, *Free Radic. Biol. Med.,* 2009, **46**, 232–237.

17

[16] A. Sosnik, D.A. Chiappetta and Á.M. Carcaboso, *J. Control. Release,* 2009, **138**, 2–15.

[17] J. Vacek, M. Zahmakıran and S. Özkar, *Nanoscale*, 2011, **3**, 3462–3481.

[18] H. I. Peng and B.L. Miller, *Analyst*, 2011, **136**, 436–447.

[19] T. K. Sau, A.L. Rogach, F. Jäckel, T.A. Klar and J. Feldmann, *Adv. Mater.,* 2010, **22**, 1805–1825.

[20] M. M. Nigra, J.M. Ha and A. Katz, *Catal. Sci. Techol.*, 2013, **3**, 2976-2983.

[21] P. Si, Y. Huang, T. Wang and J. Ma, *RSC. Adv.*, 2013, **3**, 3487-3502.

[22] S. Gupta and R. Prakash, *J. Mater. Chem. C*, 2014, **2**, 6859-6866.

[23] S. Gupta, A.K. Singh, R.K. Jain, R. Chandra and R. Prakash, Chem. Electro. Chem., 2014, **1**,793-798.

[24] R.L.J. Chang and J. Yang, *Analyst* 2011, **136**, 2988-2995.

[25] N.G. Bastus, F. Merkoci, J. Piella and V. Puntus, *Chem. Mater.* 2014, **26**, 2836-2846.

[26] S. Bayram, O.K. Zahar and A.S. Blum, *RSC Adv.* 2015, **5**, 6553-6559.

[27] N.A. Negm, S.M. Tawfik and A.A. Abd-Elaal, *J. Indus. Eng. Chem.* 2015, **25**, 1051-1057.

[28] M. Choudhary, S. Siwal, R.U. Islam, M.J. Witcomb and K. Mallick, *Chem. Phys. Lett.* 2014, **608**, 145-151.

[29] S. Zeng, D. Baillargeat, H.P. Ho and K.T. Yong, *Chem. Soc. Rev.*, 2014, **43**, 3426-3452.

[30] D. Wei, W. Sun, W. Qian, Y. Ye and X. Ma, *Carbohydrate Research*, 2009, **344**, 2375-2382.

[31] Kashish, S. Gupta, S.K. Dubey and R. Prakash, *Anal. Methods*, 2015, **7**, 2616-2622.

[32] M. Srivastava, S.K. Srivastava, N.R. Nirala and R. Prakash, *Anal. Methods,* 2014, **6**, 817-824.

[33] S. Kobayashi, K. Toshitsugu and S. Shin-ichiro, *J. Am. Chem. Soc.,* 1996, **118**, 13113-13114.

[34] K.C. Leandro, J.C. Moreira, and P.A.M. Farias , *Analytical letters*, 2010,**43**,1951-1957.

[35] K. Peckova, T. Navratil, B. Yosypchuk, J.C. Moreira, K.C. Leandro and J. Barek, *Electroanalysis* , 2009, **21**, 1750-1757.

[36] S. Mohan and R. Prakash, *Talanta,* 2010, **81**, 449-454. [37] A. A. Rafati and A. Afraz, *Mater. Sci. Eng. C,* 2014*,* **39***,* 105-112.

[37] A. A. Rafati and A. Afraz, *Mater. Sci. Eng. C,* 2014*,* **39***,* 105-112.

 [38] Z. Chen, X. Zhang, H. Cao and Y. Huang, *Analyst*, 2013, **138**, 2343-2349.

 [39] H. Huang, Q. Yuan and X. Yang, *Colloids Surf., B*, 2004, **39**, 31–37.

18

[40] C. Novo, A.M. Funston, A.K. Gooding and P. Mulvaney, *J. Am. Chem. Soc.* 2009, **131**, 14664−14666.

[41] M.F. Melendrez, G. Cardenas and J. Arbiol, *J. Colliod Interf. Sci.*, 2010, **346**, 279-287.

[42] W. Yang, Y. Ma, J. Tang and X. Yang, *Colloids Surf., A,* 2007, **302**, 628–633.

[43] Z. L. Wang, *J. Phys. Chem. B*, 2000, **104**, 1153–2117.

[44] N. Ghavale, S. Dey, V. K. Jain and R. Tewari*, Bull. Mater. Sci.,* 2009, **32**, 15–18.

[45] K.S.V.K. Rao, V.K. Naidu, M.C.S. Subha, M. Sairam and T.M. Aminabhavi, *Carbohydr. Polym.,* 2006, **66**, 333–344.

[46] K. Kalimuthu, R.S. Babu, D. Venkataraman, Md. Bilal, S. Gurunathan, *Colloid Surface B*, 2008, 65, 150-153.

[47] J. Vacek, Z. Andrysik, L. Tmkova and R. Kizek, *Electroanalysis*, 2004, **16**, 224-230.

[48] D.R. Firrer, D.H. Chidester and R.R. Schroeder, *J. Electroanal.Chem. Interf. Chem.,* 1973, **45**, 361-376.

[49] J.H. Christie and P.J. Lingane, *J. Electroanal. Chem.,* 1965, **10**, 176-182.

[50] J.J. Zipper and S.P. Perone, *Anal. Chem.*, 1973, **45**, 452-458.

[51] D.R. Firrer and R.R. Schroeder, *J. Electroanal. Chem.*, 1973, **45**, 343-359.